

Glyme–Lithium Salt Phase Behavior

Wesley A. Henderson

Department of Chemical Engineering and Materials Science, University of Minnesota,
Minneapolis, Minnesota 55455

Received: March 12, 2006

Phase diagrams are reported for glyme mixtures with simple lithium salts. The glymes studied include monoglyme (DME), diglyme, triglyme, and tetraglyme. The lithium salts include LiBETI, LiAsF₆, LiI, LiClO₄, LiBF₄, LiCF₃SO₃, LiBr, LiNO₃, and LiCF₃CO₂. The phase diagrams clearly illustrate how solvate formation and thermophysical properties are dictated by the ionic association strength of the salt (i.e., the properties of the anions) and chain length of the solvating molecules. This information provides critical predictive capabilities for solvate formation and ionic interactions common in organometallic reagents and battery electrolytes.

Introduction

Glymes, CH₃O(CH₂CH₂O)_nCH₃ (*n* = 1–4 for monoglyme–tetraglyme, respectively), are a powerful class of solvents which find wide use in organometallic reactions (Grignard, lithiations, Heck, Suzuki, Stille, McMurry), etherification of alcohols, reductions with alkali metals, alkylations with strong bases, ring rearrangements (Favorskii, Diels–Alder), hydrogenation, phase transfer catalyzed (PTC) reactions, and other reactions. As such, they are a key component of pharmaceutical and specialty chemicals production. The absence of reactive functional groups in these aprotic saturated polyethers makes them chemically inert. Most glymes are completely miscible in both water and hydrocarbon solvents. The ether oxygens (EOs) give glymes exceptional cation solvation properties often resulting in poorly solvated or “naked” active anions leading to high yields and fast reaction rates.

In recent years, it has become widely recognized that the manner in which Li⁺ cations are solvated in lithium reagents dramatically affects their reactivity and selectivity.^{1–24} Gleaning a clearer picture of why this is so requires a knowledge of the solvates present in solution. The structural characterization of amorphous systems, however, is notoriously difficult. A useful first step is to deconvolute the factors which control solvate formation via phase diagrams and determine the thermodynamically favored crystalline solvate structures. Simple lithium salts have been examined here as models for more complex organometallic reagents.

Glyme–Li⁺ cation interactions are also crucial to the performance of liquid (and solid polymer) electrolytes for electrochemical devices such as lithium batteries and light-emitting electrochemical cells. The properties of electrolytes in which ionic interactions become prominent (concentrated electrolytes) remain difficult to predict, however, as current theories do not adequately model their attributes.^{25–30} Instead, electrolyte optimization is usually by empirical means.³¹ Yet the solvates formed in electrolytes directly impact such physical properties as viscosity, ion conductivity, ion transport numbers, electrolyte vapor pressure, etc. As noted above for solutions with lithium reagents, phase diagrams and crystalline solvate structures are the key to optimizing solvent–salt mixtures for electrolyte applications.

This paper reports phase diagrams of glyme–lithium salt (LiX) mixtures. The glymes are denoted as G1 (monoglyme or

DME), G2 (diglyme), G3 (triglyme), and G4 (tetraglyme) in accord with previous reports.^{30,32} A comprehensive explanation is provided for solvate variation with different anions, as well as the thermal behavior of these solvates. Whenever possible, the phase diagrams are correlated with known glyme–LiX solvate crystal structures.

Experimental Section

Reagents were purchased from Aldrich unless otherwise noted. Anhydrous G1 and G2 were used as received. G3 and G4 were dried over 4 Å molecular sieves. The lithium salts were dried at elevated temperature under high vacuum. LiTFSI (LiN(SO₂CF₃)₂) and LiBETI (LiN(SO₂C₂F₅)₂) were kindly provided by 3M. Samples were prepared in a dry room (<0.2% relative humidity, 22 °C) and stored in desiccators. Typically, the glymes and salts were mixed together in vials and stirred while heating on a hot plate to form homogeneous solutions. It was difficult to prepare highly concentrated mixtures with LiI, LiBF₄, and LiAsF₆ using this method due to the limited thermal stability of these salts, especially with G1.

Phase diagrams were prepared from DSC heating curves (5 or 10 °C min^{−1}) using a liquid nitrogen cooled Perkin-Elmer Pyris 1 differential scanning calorimeter (DSC). Small amounts of the samples (8–25 mg) were hermetically sealed in Al pans. Often, it was necessary to heat the mixtures while stirring to form homogeneous solutions for this purpose. Sample pans were slowly cooled (−5 or −10 °C min^{−1}) from room temperature in the DSC to allow the mixtures to fully crystallize. Often there was considerable hysteresis between the crystallization and melting temperatures of the various phases (Figure 1). Some of the sample pans were stored in a freezer in hermetically sealed coffee-bag envelopes prior to analysis to further aid in crystallization. Frequently, the samples were thermally cycled or annealed for extended periods of time at low temperatures prior to analysis. The background has been subtracted from the DSC traces shown.

Results and Discussion

Neat Glymes. Glymes are flexible molecules which are able to adopt numerous conformations. G1 crystallizes readily on cooling with a subsequent melting point (mp) of −68 °C. The crystal structure of G1 is known in which the G1 molecules adopt one of two conformations (tg⁺t or tg[−]t).³³

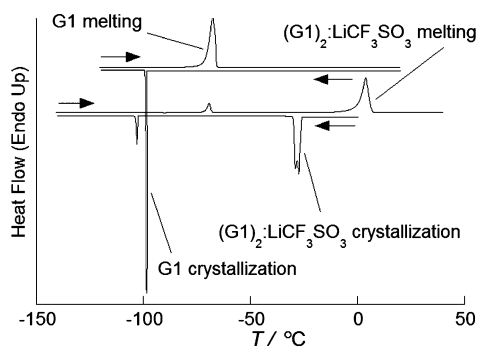
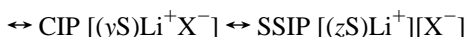


Figure 1. DSC cooling and heating traces of (top) neat G1 and (bottom) $(G1)_n\text{-LiCF}_3\text{SO}_3$ ($n = 2.3$).

Solvate Structures and Ionic Association. In dilute solutions, electrolyte mixtures are typically modeled as consisting of highly solvated “free” ions. The concentration dependence of the properties is then governed by long-range Coulombic forces as predicted by the Debye–Hückel theory. With increasing concentration, the ions begin to directly interact, and this ionic association leads to the formation of solvent-separated ion pairs (SSIP), contact ion pairs (CIP) or aggregate (AGG) solvates in which the ions are coordinated to zero, one, or more than one counterion, respectively. At even higher concentrations, the electrolyte properties may approach those of molten salts or ionic liquids.

Solvate formation for LiX salts can be represented as



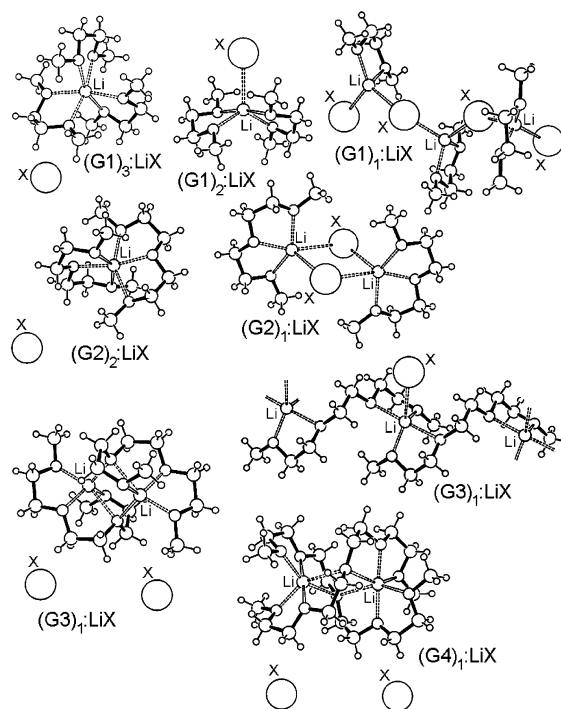
where S is a solvent donor atom (i.e., EOs), $n > m$, and $x < y < z$. Li^+ cations generally have a coordination number of 4–6 (although this can be as low as 3 and as high as 8).³⁴ An examination of known crystalline solvate structures for glyme–LiX solvates indicates that specific stoichiometric complexes are typical (Chart 1).

The ionic association strength of a salt is determined by the negative charge delocalization, size, and steric effects for a given anion. Scheme 1 summarizes an approximate ordering for increasing ionic association strength of simple LiX salts in aprotic solvents (see the Supporting Information). It will be shown below that for the same solvent (e.g., G1), the equilibrium in eq 1 will be shifted to the right principally by lowering the temperature, reducing the salt concentration, and/or using a salt with a lower ionic association strength. In fact, the solvates which form in glyme–LiX mixtures can be directly correlated with this latter property.

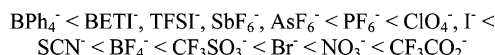
Highly Dissociated Salts. Scheme 1 indicates that, of the salts noted, LiBPh_4 is the most dissociated. LiBPh_4 is commercially sold as a SSIP $(G1)_3\text{:LiX}$ solvate, and an SSIP $(G3)_1\text{:LiX}$ solvate is known.³⁵

Dissociated Salts. Scheme 1 indicates that LiBETf and LiAsF_6 are both expected to be highly dissociated in aprotic solvents. Phase diagrams for glyme mixtures with these salts are shown in Figures 2 and 3, respectively. DSC analysis and/or partial phase diagrams have been previously reported for $(G1)_n\text{-LiBETf}$,³⁶ $(G2)_n\text{-LiBETf}$,³⁶ $(G3)_n\text{-LiBETf}$,³⁶ $(G1)_n\text{-LiTfSI}$,^{32,36,37} $(G2)_n\text{-LiTfSI}$,^{32,36,37} $(G3)_n\text{-LiTfSI}$,^{36,37} $(G4)_n\text{-LiTfSI}$,³⁷ and $(G1)_n\text{-LiAsF}_6$ ³⁸ mixtures. The structures of the SSIP $(G2)_2\text{:LiTfSI}$,³⁶ SSIP $(G2)_2\text{:LiSbF}_6$,³⁹ AGG $(G2)_{1/2}\text{:LiTfSI}$,³⁶ CIP $(G3)_1\text{:LiBETf}$,³⁶ CIP $(G3)_1\text{:LiAsF}_6$,³⁵ and SSIP $(G4)_1\text{:LiAsF}_6$ ⁴⁰ solvates are known.

CHART 1: Schematic Illustrations of Glyme–LiX Solvate Structures



SCHEME 1

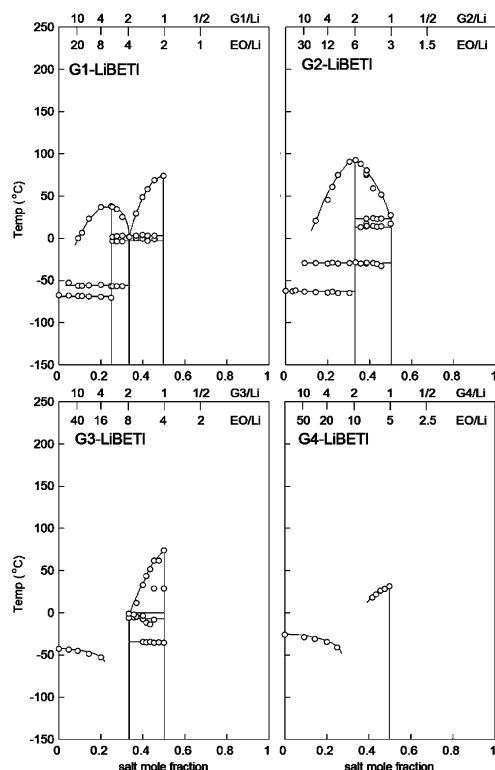
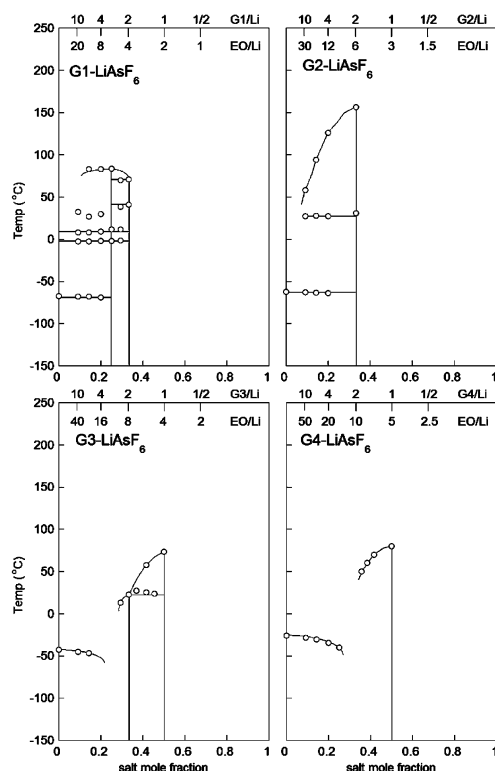


Intermediate Salts. Scheme 1 indicates that LiI , LiClO_4 , and LiBF_4 are more associated in aprotic solvents than the dissociated salts. Phase diagrams for glyme mixtures with these salts are shown in Figures 4–6, respectively. DSC analysis and/or partial phase diagrams have been previously reported for $G1\text{-LiBF}_4$,³⁸ $G1\text{-LiClO}_4$,^{41–44} and $G2\text{-LiClO}_4$ mixtures. The structures of the CIP $(G1)_2\text{:LiI}$,⁴⁵ CIP $(G1)_2\text{:LiClO}_4$,⁴⁴ CIP $(G1)_2\text{:LiBF}_4$,²⁴ SSIP $(G2)_2\text{:LiClO}_4$,⁴⁴ SSIP $(G2)_2\text{:LiBF}_4$,⁴⁶ AGG $(G2)_1\text{:LiBF}_4$,⁴⁶ CIP $(G3)_1\text{:LiClO}_4$,³⁵ CIP $(G3)_1\text{:LiBF}_4$,³⁵ and AGG $(G4)_{1/2}\text{:LiBF}_4$ ⁴⁰ solvates are known.

Associated Salts. Scheme 1 indicates that LiCF_3SO_3 and LiBr are even more associated in aprotic solvents than LiBF_4 . Phase diagrams for glyme mixtures with LiCF_3SO_3 are shown in Figure 7. A phase diagram has been previously reported for $G1\text{-LiBr}$ mixtures.^{41,42} The structures of the CIP $(G1)_2\text{:LiBr}$,^{47–49} AGG $(G1)_{1/2}\text{:LiCF}_3\text{SO}_3$,⁵⁰ AGG $(G2)_1\text{:LiCF}_3\text{SO}_3$,⁵¹ AGG $(G2)_{1/2}\text{:LiCF}_3\text{SO}_3$,⁵² CIP $(G3)_1\text{:LiCF}_3\text{SO}_3$,³⁵ AGG $(G3)_{2/3}\text{:LiCF}_3\text{SO}_3$,³⁵ and AGG $(G3)_{1/2}\text{:LiCF}_3\text{SO}_3$ ⁵⁰ solvates are known. A preliminary structure for an AGG $(G4)_{1/3}\text{:LiCF}_3\text{SO}_3$ ⁴⁰ has also been reported.

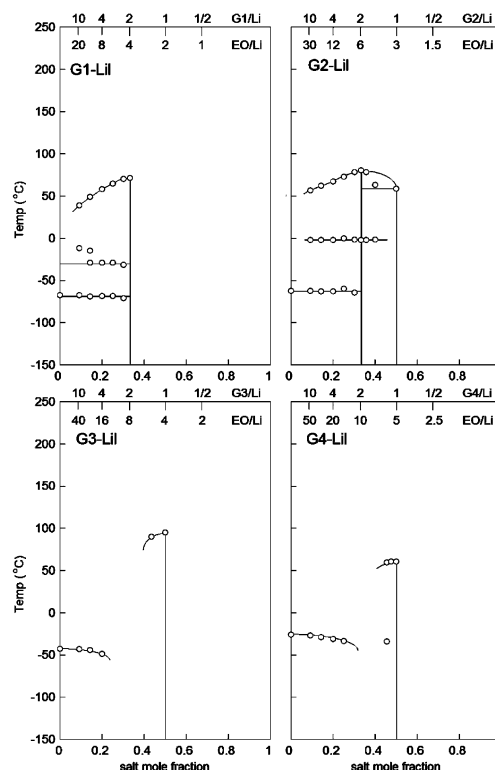
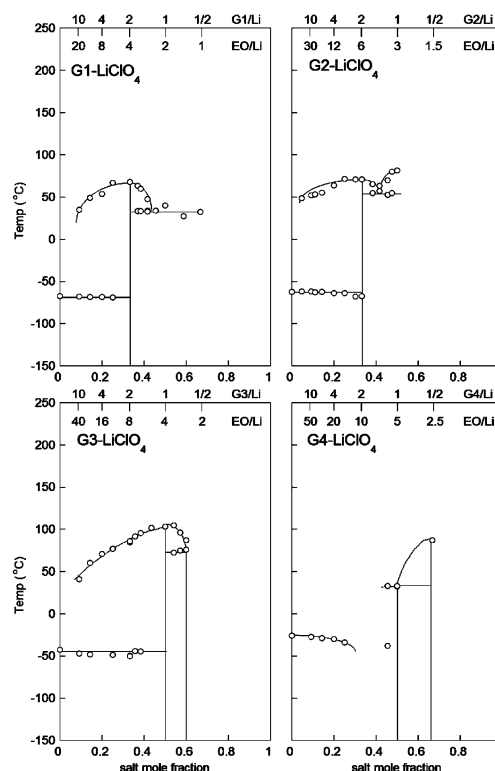
Highly Associated Salts. Scheme 1 indicates that LiNO_3 and LiCF_3CO_2 are even more associated in aprotic solvents than LiCF_3SO_3 . Phase diagrams for glyme mixtures with these salts are shown in Figures 8 and 9, respectively. The structures of the AGG $(G1)_1\text{:LiNO}_3$,⁵³ AGG $(G2)_{1/3}\text{:LiCF}_3\text{CO}_2$,⁵² and AGG $(G4)_{2/5}\text{:LiCF}_3\text{CO}_2$ ⁴⁰ solvates are known.

Solvate Stability. It is instructive to examine which of the crystalline phases is the first to form (with increasing salt concentration) for a given (glyme)_n–LiX mixture. Clearly the dissociated salts (i.e., LiBPh_4 , LiBETf , LiTfSI , and LiAsF_6) form SSIP solvates preferentially when enough solvent donor atoms are available for Li^+ cation coordination (Table 1). At

Figure 2. Phase diagrams of (glyme)_n-LiBETI mixtures.Figure 3. Phase diagrams of (glyme)_n-LiAsF₆ mixtures.

the opposite extreme are the highly associated salts. LiCF₃CO₂ does not form any SSIP solvates and only a single CIP solvate. A strong correspondence therefore exists between the ionic association strength of the LiX salts (Scheme 1) and the solvate phase behavior (Table 1).

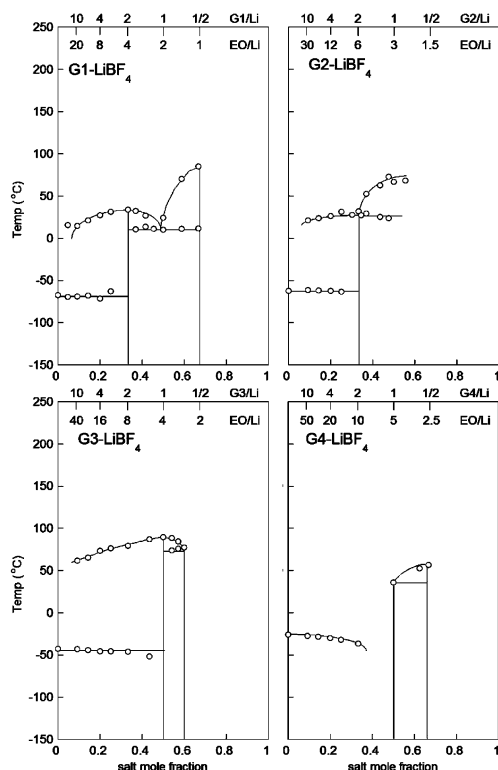
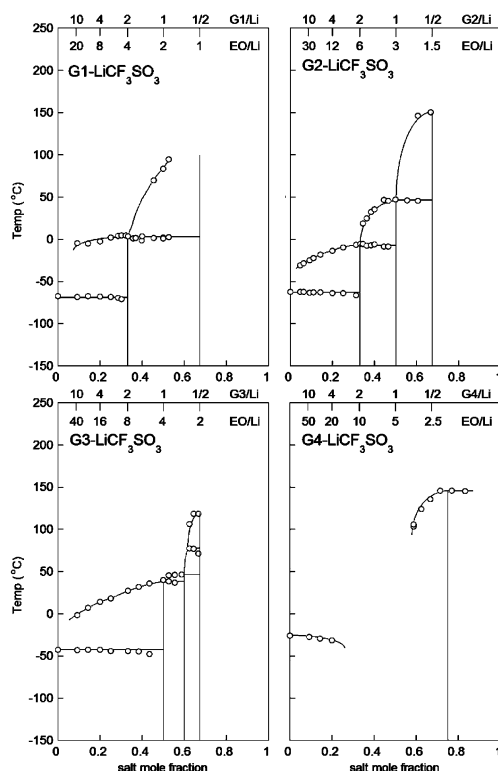
One may go a step further and note that the thermal stability of the SSIP and CIP solvates is also linked with the ionic association strength of the LiX salts. For example, the mp's of

Figure 4. Phase diagrams of (glyme)_n-LiI mixtures.Figure 5. Phase diagrams of (glyme)_n-LiClO₄ mixtures.

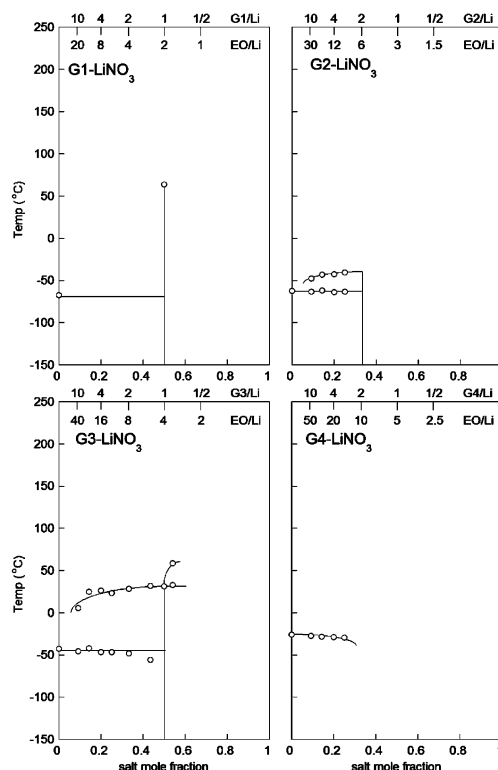
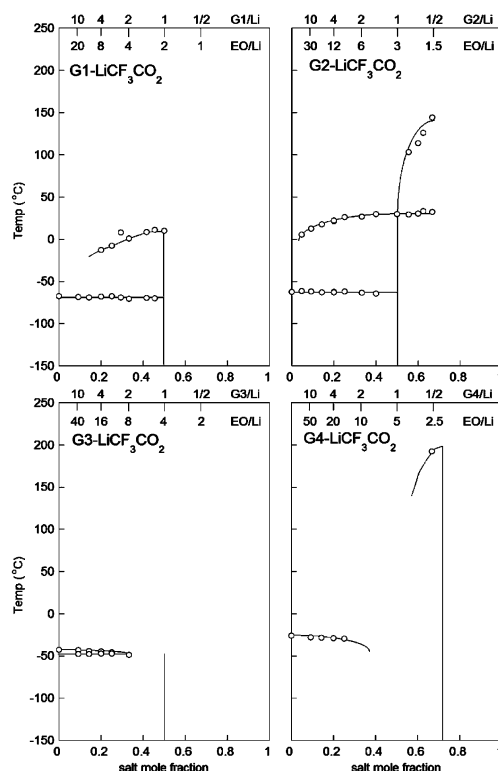
the SSIP (G2)₂:LiX and CIP (G3)₁:LiX solvates increase as



There are two probable mechanisms for the melting of the crystalline solvates. In the first, increasing thermal energy disrupts the ordered packing of the solvate, but the basic local structure is retained in the liquid phase. Alternatively, thermal

Figure 6. Phase diagrams of (glyme)_n-LiBF₄ mixtures.Figure 7. Phase diagrams of (glyme)_n-LiCF₃SO₃ mixtures.

energy may weaken the EO...Li⁺ cation coordination leading to the displacement of one or more of the coordinating EOs from the glyme molecules by the donor atoms of the neighboring anions resulting in the formation of more associated amorphous solvates. As the ionic association strength of a salt increases, there will be a shift from the former to the latter mechanism. Thus, once theSSIP (G1)₃:LiTFSI phase melts, a large fraction of [(G1)₃Li]⁺ cations and neighboring uncoordinated TFSI⁻ anions (i.e., SSIPs) are still present, but packed together in a

Figure 8. Phase diagrams of (glyme)_n-LiNO₃ mixtures.Figure 9. Phase diagrams of (glyme)_n-LiCF₃CO₂ mixtures.

disordered manner. This is supported by vibrational spectroscopy studies of the solutions (see the Supporting Information).³⁷ In contrast, as the CIP (G1)₂:LiCF₃SO₃ phase melts, a large fraction of AGGs form (see the Supporting Information).⁴⁷ The same holds for (G2)₂:LiX solvates with LiPF₆ and LiClO₄.⁵⁴ This relationship between ionic association strength and thermal stability, however, must be used with caution. Other factors also affect solvate stability. In particular, the high flexibility of anions such as TFSI⁻ and BETI⁻ results in thermal motions which may

TABLE 1: First Crystalline Solvates to Form (with Increasing Salt Concentration) in Glyme–LiX Mixtures

	G1			G2		G3			G4		
	3/1 (SSIP)	2/1 (CIP)	1/1 (AGG)	2/1 (SSIP)	1/1 (AGG)	2/1 (SSIP)	1/1 (SSIP)	1/1 (CIP)	1/1 (SSIP)	1/3 (AGG)	2/5 (AGG)
LiBPh ₄	x						x				
LiBETI	x			x		x			x		
LiTFSI	x			x							
LiAsF ₆	x			x		x			x		
LiI		x		x			x	x	x		
LiClO ₄		x		x			x	x	x		
LiBF ₄		x		x			x	x	x		
LiCF ₃ SO ₃		x		x			x			x	
LiBr		x		x							
LiNO ₃		x		x			x				
LiCF ₃ CO ₂			x		x		x				x

aid in disrupting the solvate crystal packing and thus reduce the mp. In addition, bulky anions such as BETI[−] may form solvates with very different structures, but equivalent stoichiometries (i.e., CIP (G3)₁:LiBETI vs (G3)₁:LiAsF₆)^{35,36} due to steric effects.

Which crystalline solvates have the highest thermodynamic stability (i.e., lowest free energy)? Of the SSIP solvates, the (G2)₂:LiX solvate is the most stable since it is present for all of the salts except LiCF₃CO₂ and the mp is the highest of the SSIP solvates for a given salt. This arises from the favorable coordination of the Li⁺ cations by six EOs, all with short coordination bond distances (typical EO–Li distances ~2.0–2.3 Å).^{39,44,46} The (G1)₃:LiX solvate, however, also consists of Li⁺ cations coordinated by six EOs, also with short coordination bond distances (typical EO–Li distances ~2.0–2.2 Å).^{55–57} A clear distinction exists, however, between the thermal stability of these two solvates, with the mp's of the G1 solvates much lower than those with G2. How can this be explained? In general, an ionic coordination bond is not a static thing, but rather the strength, as reflected in the length of this bond, varies with thermal fluctuations and steric interactions with neighboring atoms. Thus, ionic coordination bonds to a given Li⁺ cation are made, broken, and reformed with the same or different EO donor atoms. The rate at which this occurs increases with increasing temperature. The probability that these bonds are reformed with the same rather than a different donor atom (donor exchange) increases significantly if the donor atom is physically attached to another donor atom coordinating the same Li⁺ cation. The remaining coordinating atom hinges the original donor atom in the vicinity of the cation making the reformation of a bond more probable while simultaneously hindering neighboring solvent molecules from approaching the cation. Solvent exchange thus occurs more slowly for multidentate ligands. G1 is therefore expected to be better at Li⁺ cation coordination than THF and G2 is better than G1 explaining the stability differences noted above (see the Supporting Information). This is born out by experimental observations^{17,58} and explains why glymes are found to preferentially solvate Li⁺ cations over other solvents with higher permittivities.^{59–65}

The CIP (G3)₁:LiX solvates are thermodynamically more favorable than the CIP (G1)₂:LiX solvates, as indicated by the higher mp's of the former. This is attributed to the polymeric rather than monomeric structure of the (G3)₁:LiX solvates since the coordination about the Li⁺ cations is very similar in both cases.^{35,44}

Although the (G3)₁:LiBPh₄ solvate³⁵ demonstrates that it is possible to form an SSIP solvate with a 1:1 G3:Li stoichiometry,

all of the other (G3)₁:LiX solvates are CIPs, even those with LiAsF₆ and LiBETI.^{35,36} The SSIP (G3)₁:LiX dimer solvate formed with LiBPh₄ consists of two Li⁺ cations each coordinated to four EOs from a single G3 (EO–Li distances ~2.0 Å) and a fifth EO from a second G3 (EO–Li distances ~2.3–2.4 Å). This weak fifth coordinating bond explains why only the very poorly coordinating BPh₄[−] anion does not form a CIP solvate since this position can be easily exchanged with an anion donor atom. These differences in solvate formation and stability permit a demarcation of the salts into the categories noted above.

Solid–Solid Phase Transitions. Many of the solvates have endothermic features prior to the melting transition. These likely correspond to solid–solid phase transitions in which some or all of the anions or solvated cations become disordered forming plastic crystalline phases. Orientational disorder is well-known in salts with anions such as ClO₄[−], BF₄[−], and PF₆[−].^{66–68} The (G2)₂:LiPF₆ solvate has a solid–solid phase transition at 22 °C.⁵⁴ Vibrational spectroscopy suggests that only minor changes in Li⁺ cation coordination occur in this latter solvate above this transition implying that it is the PF₆[−] anions which become disordered, perhaps in the manner of SbF₆[−] anions in the (G2)₂:LiSbF₆ crystalline solvate.³⁹ In addition to rotational disorder, anions such as TFSI[−] can also become conformationally disordered in the solid state.^{69,70}

Crystallinity Gaps. Composition regions exist in several of the phase diagrams in which it was not possible to crystallize the mixtures, so-called “crystallinity gaps” To explain this, it is important to note that the nucleation and growth of ordered crystalline phases is slowed or inhibited altogether when the local structure in the amorphous phase does not resemble that of the crystalline state.

For the dissociated salts, it was not possible to crystallize the SSIP (G3)₂:LiX solvate for (G3)_{*n*}:LiX mixtures with *n* > 2–2.2 (some G3 does crystallize in dilute mixtures) (see the Supporting Information). Crystallization kinetics for this phase are slow, however, even when *n* ≤ 2. As yet, there are no known crystal structures for (G3)₂:LiX solvates, but (G3)₂:NaX solvates are SSIPs with all eight EOs coordinated to the Na⁺ cations.^{71–75} It is possible for all four EOs of a G3 molecule to coordinate a single Li⁺ cation in a crown ether-like conformation.³⁶ The (G3)₂:LiX solvates, therefore, probably resemble (12-crown-4)₂:LiX solvates such as (12-crown-4)₂:LiTFSI.⁷⁶ Such solvates, however, have weak (i.e., long) coordination bonds (eight EO–Li distances 2.3–2.5 Å). One explanation for the crystallinity gaps is that in the amorphous phase, the Li⁺ cations are coordinated to fewer EOs, but with stronger (i.e., shorter) coordination bonds (similar to the (G2)₂:LiX solvate) leaving uncoordinated EOs on the glymes. Steric interactions with neighboring uncoordinated glyme molecules and thermal energy may hinder or prevent the crown ether-like coordination required for the crystalline solvate.

The crystallinity gap for (G4)_{*n*}:LiCF₃SO₃ mixtures (Figure 10) is explained by the fact that a SSIP (G4)₁:LiCF₃SO₃ phase does not form since such mixtures consist predominantly of CIPs and AGGs (see the Supporting Information), with most of the AGG anions coordinated to two, rather than three, Li⁺ cations.⁴⁷ The anions in the crystalline AGG (G4)_{1/3}:LiCF₃SO₃ solvate, however, are coordinated to either two or three cations.⁴⁰ Thus, the amorphous phase resembles neither the SSIP phase found with less associating anions, nor the AGG phase found in much more concentrated mixtures (where less EOs are available for cation coordination).

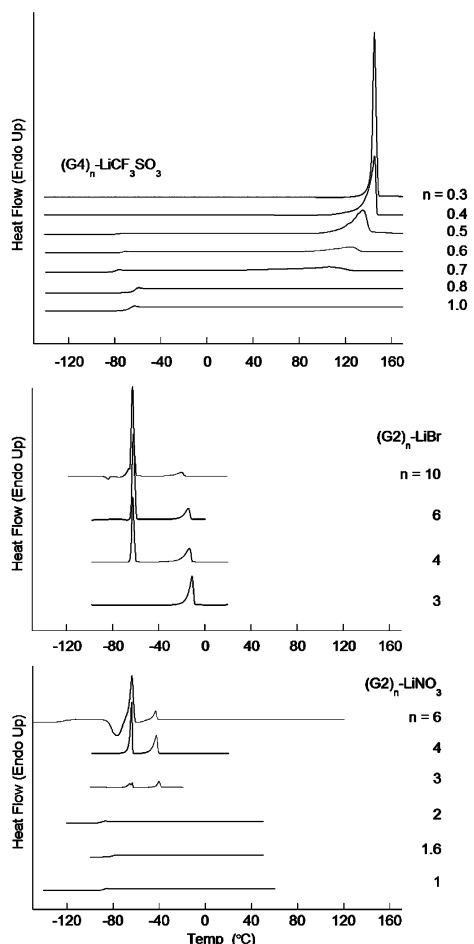


Figure 10. DSC heating traces of $(G4)_n$ -LiCF₃SO₃, $(G2)_n$ -LiBr, and $(G2)_n$ -LiNO₃ mixtures.

Crystallinity gaps also occur for more strongly associating salts. For example, in dilute $(G2)_n$ -LiX mixtures with LiBr and LiNO₃, it is possible to crystallize a $(G2)_2$ -LiX phase (Figure 10), but the nucleation and growth of this phase with these salts is extremely slow (several hours of slowly cycling at low temperatures is required for crystallization). Interestingly, as the salt concentration increased (approaching $n = 2$), it became more difficult to crystallize the samples, in particular the $(G2)_2$ -LiNO₃ phase. This can be explained by a low fraction of SSIPs in dilute mixtures, which decreases further with increasing salt concentration.

Note that it is not appropriate to state with certainty that a given phase cannot be formed. It may simply be a matter of improper experimental conditions for crystallization due to slow kinetics. The crystallinity gap in $(G3)_n$ -LiI mixtures suggests that it may be possible to crystallize a SSIP $(G3)_2$ -LiI phase. Small endothermic peaks not attributed to solid–solid phase transitions were also found in dilute $(G1)_n$ -LiX mixtures with LiI, LiClO₄, and LiCF₃SO₃ which may indicate that a SSIP $(G1)_3$ -LiX phase can be formed at low temperatures. If such phases form, their nucleation and growth is extremely sluggish. An examination of the crystallization kinetics of these glyme–LiX mixtures would be complementary to the present study and very informative.

Conclusions

Phase diagrams are reported for monoglyme, diglyme, triglyme, and tetraglyme mixtures with a variety of lithium salts. The solvate phases formed and thermal properties of the phases

have been scrutinized enabling the development of a comprehensive picture of the molecular interactions in these glyme–salt mixtures based upon the ionic association strength of the salt.

Acknowledgment. W.A.H. is indebted to the National Science Foundation for the award of an NSF Graduate Research Fellowship and the University of Minnesota for a Graduate Research Fellowship.

Supporting Information Available: Tabulated relative salt ionic association strength information and DSC heating traces of glyme–LiX mixtures (pdf). This material is available free of charge via the Internet at <http://pubs.acs.org>.

References and Notes

- (1) Yakimansky, A. V.; Müller, A. H. E. *J. Am. Chem. Soc.* **2001**, *123*, 4932.
- (2) Lucht, B. L.; Bernstein, M. P.; Remenar, J. F.; Collum, D. B. *J. Am. Chem. Soc.* **1996**, *118*, 10707.
- (3) Lucht, B. L.; Collum, D. B. *Acc. Chem. Res.* **1999**, *32*, 1035.
- (4) Lucht, B. L.; Collum, D. B. *J. Am. Chem. Soc.* **1996**, *118*, 2217.
- (5) Rutherford, J. L.; Collum, D. B. *J. Am. Chem. Soc.* **2001**, *123*, 199.
- (6) Rutherford, J. L.; Collum, D. B. *J. Am. Chem. Soc.* **1999**, *121*, 10198.
- (7) Gschwind, R. M.; Rajamohanam, P. R.; John, M.; Boche, G. *Organometallics* **2000**, *19*, 2868.
- (8) Henderson, K. W.; Dorigo, A. E.; Liu, Q.-Y.; Williard, P. G. *J. Am. Chem. Soc.* **1997**, *119*, 11855.
- (9) Pauls, J.; Neumüller, B. *Inorg. Chem.* **2001**, *40*, 121.
- (10) Böck, S.; Nöth, H.; Rahm, P. Z. *Naturforsch., B: Chem. Sci.* **1988**, *43*, 53.
- (11) Linti, G.; Nöth, H.; Rahm, P. Z. *Naturforsch., B: Chem. Sci.* **1988**, *43*, 1101.
- (12) Deacon, G. B.; Forsyth, C. M.; Scott, N. M. *Dalton Trans.* **2001**, 2494.
- (13) Nöth, H.; Thomas, S.; Schmidt, M. *Chem. Ber.* **1996**, *129*, 451.
- (14) Giese, H.-H.; Nöth, H.; Schwenk, H.; Thomas, S. *Eur. J. Inorg. Chem.* **1998**, 941.
- (15) Giese, H.-H.; Habereeder, T.; Nöth, H.; Ponikvar, W.; Thomas, S.; Warchhold, M. *Inorg. Chem.* **1999**, *38*, 4188.
- (16) Casado, F.; Pisano, L.; Farriol, M.; Gallardo, I.; Marquet, J.; Melloni, G. *J. Org. Chem.* **2000**, *65*, 322.
- (17) John, M.; Auel, C.; Behrens, C.; Marsch, M.; Harms, K.; Bosold, F.; Gschwind, R. M.; Rajamohanam, P. R.; Boche, G. *Chem.—Eur. J.* **2000**, *6*, 3060.
- (18) Reich, H. J.; Green, D. P.; Medina, M. A.; Goldenberg, W. S.; Gudmundsson, B. Ö.; Dykstra, R. R.; Phillips, N. H. *J. Am. Chem. Soc.* **1998**, *120*, 7201.
- (19) Reich, H. J.; Borst, J. P.; Dykstra, R. R.; Green, D. P. *J. Am. Chem. Soc.* **1993**, *115*, 8728.
- (20) Reich, H. J.; Goldenberg, W. S.; Gudmundsson, B. Ö.; Sanders, A. W.; Kulicke, K. J.; Simon, K.; Guzei, I. A. *J. Am. Chem. Soc.* **2001**, *123*, 8067.
- (21) Andrianarison, M. M.; Avent, A. G.; Ellerby, M. C.; Gorrell, I. B.; Hitchcock, P. B.; Smith, J. D.; Stanley, D. R. *Dalton Trans.* **1998**, 249.
- (22) Wang, J. S.; Jérôme, R.; Warin, R.; Zhang, H.; Teyssié, Ph. *Macromolecules* **1994**, *27*, 3376.
- (23) Seebach, D. *Angew. Chem., Int. Ed. Engl.* **1988**, *27*, 1624.
- (24) Ramírez, A.; Lobkovsky, E.; Collum, D. B. *J. Am. Chem. Soc.* **2003**, *125*, 15376.
- (25) Chen, Z.; Hojo, M. *J. Phys. Chem. B* **1997**, *101*, 10896.
- (26) Salomon, M. *J. Solution Chem.* **1993**, *22*, 715.
- (27) Balkowska, A.; Szymański, G.; Werblan, L. J. *Electroanal. Chem.* **1990**, *287*, 229.
- (28) Chagnes, A.; Carré, B.; Willmann, P.; Lemordant, D. *J. Power Sources* **2002**, *109*, 203.
- (29) Ue, M. *J. Electrochem. Soc.* **1994**, *141*, 3336.
- (30) Brouillette, D.; Perron, G.; Desnoyers, J. E. *Electrochim. Acta* **1999**, *44*, 4721.
- (31) Dudley, J. T.; Wilkinson, D. P.; Thomas, G.; LeVae, R.; Woo, S.; Blom, H.; Horvath, C.; Juzkow, M. W.; Denis, B.; Juric, P.; Aghakian, P.; Dahn, J. R. *J. Power Sources* **1991**, *35*, 59.
- (32) Choquette, Y.; Brisard, G.; Parent, M.; Brouillette, D.; Perron, G.; Desnoyers, J. E.; Armand, M.; Gravel, D.; Slougui, N. *J. Electrochem. Soc.* **1998**, *145*, 3500.
- (33) Yokoyama, Y.; Uekusa, H.; Ohashi, Y. *Chem. Lett.* **1996**, 443.

- (34) Olsher, U.; Izatt, R. M.; Bradshaw, J. S.; Dalley, N. K. *Chem. Rev.* **1991**, *91*, 137.
- (35) Henderson, W. A.; Brooks, N. R.; Brennessel, W. W.; Young, V. G., Jr. *Chem. Mater.* **2003**, *15*, 4679.
- (36) Henderson, W. A.; McKenna, F.; Khan, M. A.; Brooks, N. R.; Young, V. G., Jr.; Frech, R. *Chem. Mater.* **2005**, *17*, 2284.
- (37) Brouillette, D.; Irish, D. E.; Taylor, N. J.; Perron, G.; Odziemkowski, M.; Desnoyers, J. E. *Phys. Chem. Chem. Phys.* **2004**, *4*, 6063.
- (38) Goncharova, I. V.; Plakhotnik, V. N.; Kovtun, Y. V. *Russ. J. Inorg. Chem. (Engl. Transl.)* **1999**, *44*, 979.
- (39) Seneviratne, V.; Frech, R.; Furneaux, J. E.; Khan, M. *J. Phys. Chem. B* **2004**, *108*, 8124.
- (40) Henderson, W. A.; Brooks, N. R.; Young, V. G., Jr. *Chem. Mater.* **2003**, *15*, 4685.
- (41) Perron, G.; Couture, L.; Lambert, D.; Desnoyers, J. E. *J. Electroanal. Chem.* **1993**, *355*, 277.
- (42) Couture, L.; Desnoyers, J. E.; Perron, G. *Can. J. Chem.* **1996**, *74*, 153.
- (43) Il'in, K.; Demakhin, A. G. *Izv. Vyssh. Uchebn. Zaved., Khim. Khim. Tekhnol.* **1998**, *41*, 38.
- (44) Henderson, W. A.; Brooks, N. R.; Brennessel, W. W.; Young, V. G., Jr. *J. Phys. Chem. A* **2004**, *108*, 225.
- (45) Riffel, H.; Neumüller, B. *Fluck, E. Z. Anorg. Allg. Chem.* **1993**, *619*, 1682.
- (46) Andreev, Y. G.; Seneviratne, V.; Khan, M.; Henderson, W. A.; Frech, R. E.; Bruce, P. G. *Chem. Mater.* **2005**, *17*, 767.
- (47) Huang, W. Ph.D. Thesis, The University of Oklahoma, 1994.
- (48) Becker, G.; Eschbach, B.; Mundt, O.; Reti, M.; Niecke, E.; Issberner, K.; Nieger, M.; Thelen, V.; Nöth, H.; Waldhör, R.; Schmidt, M. *Z. Anorg. Allg. Chem.* **1998**, *624*, 469.
- (49) Rogers, R. D.; Bynum, R. V.; Atwood, J. L. *J. Crystallogr. Spectrosc. Res.* **1984**, *14*, 29.
- (50) Frech, R.; Rhodes, C. P.; Khan, M. *Macromol. Symp.* **2002**, *186*, 41.
- (51) Rhodes, C. P.; Frech, R. *Macromolecules* **2001**, *34*, 2660.
- (52) Henderson, W. A.; Young, V. G., Jr.; Brooks, N. R.; Smyrl, W. H. *Acta Crystallogr.* **2002**, *C58*, m501.
- (53) Henderson, W. A.; Brooks, N. R.; Smyrl, W. H. *Acta Crystallogr.* **2002**, *E58*, m500.
- (54) Grondin, J.; Ducasse, L.; Bruneel, J.-L.; Servant, L.; Lassègues, J.-C. *Solid State Ionics* **2004**, *166*, 441.
- (55) Näther, C.; Bock, H. *Acta Crystallogr.* **1995**, *C51*, 2510.
- (56) Schumann, H.; Nickel, S.; Loebel, J.; Pickardt, J. *Organometallics* **1988**, *7*, 2004.
- (57) Näther, C.; Bock, H.; Havlas, Z.; Hauck, T. *Organometallics* **1998**, *17*, 4707.
- (58) Firman, P.; Xu, M.; Eyring, E. M.; Petrucci, S. *J. Phys. Chem.* **1993**, *97*, 3606.
- (59) Ishikawa, M.; Wen, S.-Q.; Matsuda, Y. *J. Power Sources* **1993**, *45*, 229.
- (60) Gores, H. J.; Barthel, J. *J. Solution Chem.* **1980**, *9*, 939.
- (61) Morita, M.; Asai, Y.; Yoshimoto, N.; Ishikawa, M. *J. Chem. Soc., Faraday Trans.* **1998**, *94*, 3451.
- (62) Matsuda, Y.; Nakashima, H.; Morita, M.; Takasu, Y. *J. Electrochem. Soc.* **1981**, *128*, 2552.
- (63) Matsuda, Y.; Morita, M.; Tachihara, F. *Bull. Chem. Soc. Jpn.* **1986**, *9*, 1967.
- (64) Chintapalli, S.; Frech, R. *Solid State Ionics* **1996**, *86–88*, 341.
- (65) Frech, R.; Chintapalli, S. *Solid State Ionics* **1996**, *85*, 61.
- (66) Palacios, E.; Burriel, R.; Ferloni, P. *Acta Crystallogr.* **2003**, *B59*, 625.
- (67) Ishida, H.; Nakai, T.; Kumagai, N.; Kubozono, Y.; Kashino, S. *J. Mol. Struct.* **2002**, *606*, 273.
- (68) Bu, X.; Cisarova, I.; Coppens, P. *Acta Crystallogr.* **1992**, *C48*, 1562.
- (69) Johansson, P.; Gejji, S. P.; Tegenfeldt, J.; Lindgren, J. *Electrochim. Acta* **1998**, *43*, 1375.
- (70) Henderson, W. A.; Herstedt, M.; Young, V. G., Jr.; Passerini, S.; De Long, H. C.; Trulove, P. C. *Inorg. Chem.* **2006**, *45*, 1412.
- (71) Bock, H.; Sievert, M.; Bogdan, C. L.; Kolbesen, B. O.; Wittershagen, A. *Organometallics* **1999**, *18*, 2387.
- (72) Bock, H.; Näther, C.; Havlas, Z. *J. Am. Chem. Soc.* **1995**, *117*, 3869.
- (73) Bock, H.; Näther, C.; Havlas, Z.; John, A.; Arad, C. *Angew. Chem., Int. Ed. Engl.* **1994**, *33*, 875.
- (74) Noordik, J. H.; Beurskens, P. T.; van den Hark, T. E. M.; Smits, J. M. M. *Acta Crystallogr.* **1979**, *B35*, 621.
- (75) Bock, H.; Hauck, T.; Näther, C.; Havlas, Z. *Z. Naturforsch., B: Anorg. Chem., Org. Chem., Biochem., Biophys., Biol.* **1997**, *52*, 524.
- (76) Dillon, R. E. A.; Stern, C. L.; Shriver, D. F. *Solid State Ionics* **2000**, *133*, 247.